

Closed form logical error rate approximations for surface codes

Shaked Regev^a, Daniel Dilley^b, Andrea Delgado^a, Ryan Bennink^a

^aOak Ridge National Laboratory, 1 Bethel Valley Road, Oak Ridge, Tennessee, USA

^bArgonne National Laboratory, 9700 S Cass Ave, Lemont, Illinois, USA

ARTICLE HISTORY

Compiled May 6, 2026

ABSTRACT

We propose a novel method to calculate logical error rates in surface codes, assuming independent and identically distributed physical errors. We show how to use our method to analyze hypothetical quantum computers with various configurations and select designs with lower error rates. Currently, this requires expensive classical simulations of quantum decoders for various distances and physical error rates or inaccurate extrapolation from minimal experimental data. Instead, we use the symmetry of the problem to count the configurations that result in a logical error with our novel software. Given a physical error rate, we can deduce the probability of a logical error, to provably good accuracy. We include an analysis of measurement errors to allow a more complete comparison of different surface code implementations.

KEYWORDS

code distance, combinatorics, quantum error correction, path counting, surface code, rotated code

1. Introduction

Despite advances in high-performance computing, many scientifically significant problems remain intractable for classical algorithms due to their exponentially increasing runtime or memory requirements. Some quantum algorithms improve this scaling substantially [9], but practical, large-scale implementations remain beyond current technological capabilities. One major challenge in realizing fault-tolerant quantum computation is that quantum bits (qubits) are far noisier than classical bits.

Currently, some qubit platforms have error rates on the order of 10^{-4} in idealized settings, but there is no indication that this can be improved or even maintained at scale. Since most useful quantum algorithms require thousands of qubits and millions of sequential gate operations, even small physical error rates compound rapidly, meaning a naive implementation would be untrustworthy. This motivates developing and using

Approved for Public Release, Distribution Unlimited

Disclaimer: The views, opinions, and/or findings expressed are those of the authors and should not be interpreted as representing the official views or policies of DARPA or the U.S. Government.

Notice: This manuscript has been authored by UT-Battelle, LLC, under contract DE-AC05-00OR22725 with the US Department of Energy (DOE). The US government retains and the publisher, by accepting the article for publication, acknowledges that the US government retains a nonexclusive, paid-up, irrevocable, worldwide license to publish or reproduce the published form of this manuscript, or allow others to do so, for US government purposes. DOE will provide public access to these results of federally sponsored research in accordance with the DOE Public Access Plan (<https://www.energy.gov/doe-public-access-plan>).

quantum error correction (**QEC**) techniques to reduce effective error rates.

QEC enables fault-tolerant quantum computation by encoding information in a logical qubit using multiple physical qubits. This protects the data from decoherence and gate imperfections. The quantum information is distributed non-locally, so that local errors can be detected and corrected before they accumulate into logical failures. In this framework, a single logical qubit is represented by an entangled subspace of several qubits, typically stabilized by a set of commuting operators that detect errors without disturbing the encoded state.

The state of a pure qubit can be parameterized by two angles θ, ϕ on the Bloch sphere. A general state $|\psi\rangle$ can be written as $|\psi\rangle = \cos(\theta/2)|0\rangle + e^{i\phi}\sin(\theta/2)|1\rangle$. The standard computational basis for a single qubit is given by the vectors $|0\rangle = \{1, 0\}$ and $|1\rangle = \{0, 1\}$. An error in θ corresponds to a bit-flip (X) error, which mixes the computational basis states, whereas an error in ϕ corresponds to a phase-flip (Z), which introduces a relative phase on the $|1\rangle$ state. One can show that any other single-qubit error is a combination of these two. Further details of this are beyond the scope of the paper. We refer the reader to [10] and references therein.

The logical states $|0_L\rangle$ and $|1_L\rangle$ are the encoded analogues of the computational basis states $|0\rangle$ and $|1\rangle$. They form the basis of a protected logical subspace in which quantum algorithms operate as though they were manipulating the ideal qubit. A logical error occurs when a combination of errors on the physical qubits collectively mimics the action of a logical operator on this subspace, thereby flipping or dephasing the logical qubit and corrupting the encoded information. Such events cannot be corrected by the code's stabilizers because they act nontrivially within the logical subspace itself.

The fewest physical qubit errors that can cause this logical failure is a function of the code distance d . Specifically, a logical error arises when at least $d_e = \lceil d/2 \rceil$ physical qubits along a critical path are affected. This means that odd d is more efficient than even d for correcting errors. So, we focus on odd d and redefine $d_e \doteq (d + 1)/2$. For sufficiently low physical error rates $p < p_{th}$, where p_{th} is the surface code threshold, the logical error rate decreases exponentially with d [4].

The planar surface code [7] is one of the most widely studied and accessible QEC codes. Its topological nature and reliance on only nearest-neighbor interactions make it particularly well suited for many quantum architectures. It encodes logical qubits using a two-dimensional array of physical qubits. Stabilizer measurements detect X or Z -errors. We consider the unrotated and rotated variants of planar codes.

An *unrotated surface code* is the standard planar surface code, where physical qubits are arranged on a square lattice, with stabilizers defined over plaquettes to detect both errors. Logical operators act on the encoded qubit as a whole. The logical X operator X_L is implemented by applying X operators along a vertical chain of qubits spanning the lattice. The logical Z operator Z_L corresponds to a horizontal chain of Z operators. These operators commute with all stabilizers, but act nontrivially on the logical subspace, performing the logical bit-flip $|0_L\rangle \leftrightarrow |1_L\rangle$ or applying the logical phase-flip $|1_L\rangle \rightarrow -|1_L\rangle$. For unrotated surface codes, a chain of d_e physical qubit errors along a row or column suffices to generate a logical error.

A *rotated surface code* [2, 6] is obtained by rotating the planar lattice 45° . This reduces the number of physical qubits required for a given d by a factor of almost 2, while preserving QEC capabilities. In this geometry, logical operators traverse zig-zag minimum-length paths connecting the lattice boundaries. X_L operators propagate from top to bottom, and Z_L operators propagate from left to right. The rotated lattice imposes constraints on the possible configurations of physical qubits along these paths. Multiple minimum-length logical paths (MLLPs) may exist for the same logical opera-

tor. So for a given d rotated codes have higher error rates. Overall, the tradeoff is such that rotated codes require $\approx 75\%$ of unrotated codes to achieve similar accuracy [11].

A plaquette in the surface code is a stabilizer generator associated with a square face of the lattice. For instance, in the rotated code shown in Figures 1 and 2, a single syndrome qubit is on the face of each plaquette and the data qubits are on the vertices. For the X -type plaquette (pink), the X -stabilizers are implemented by preparing the syndrome qubit in the state $|+\rangle = (1/\sqrt{2})(|0\rangle + |1\rangle)$, applying a CNOT gate from that qubit to each data qubit, and then measuring in the X -basis ($|+/-\rangle$). These detect the phase-flip errors. The process is identical with Z -type plaquettes (green), except the syndrome qubit is initiated in the $|0\rangle$ state and the measurement is made in the Z -basis ($|0/1\rangle$). These will detect the bit-flip errors.

Surface code decoders process stabilizer measurement outcomes (syndromes) to infer most likely configurations of physical errors. A perfect decoder can correct any set of physical errors affecting up to $(d-1)/2 = d_e - 1$ qubits. Logical errors arise when different physical error configurations produce identical syndromes, causing the decoder to apply the wrong correction. This effect is particularly significant in rotated surface codes, where overlapping MLLPs may share syndromes, and distinct physical error patterns become indistinguishable to the decoder.

To design a practical quantum computer and assess its reliability, one must currently simulate every combination of p and d of interest. This is prohibitively expensive, particularly for small p and large d . An alternative is simulating a few points and extrapolating the rest, but this is inaccurate in the same regime [5]. Neither method can accurately capture the behavior of large-scale quantum systems in reasonable time.

Our framework allows analysis of logical error rates in unrotated and rotated surface codes. We first systematically enumerate error configurations along MLLPs for any d . We can then combine this with any p and can compute approximation to L efficiently. Our approach is provably accurate in regimes of interest and avoids resource-intensive simulations. It gives a rigorous upper bound on the quality of QEC for any imaginable surface code configuration within a minute of serial run time.

We assume that (i) our decoder is classical and perfect, (ii) unless stated otherwise, physical errors are independent (in space and time) and identically distributed (**i.i.d**) Pauli errors, i.e. they are Markovian, and (iii) measurement errors take a certain form (see Section 4). Table 1 summarizes the notation used in the bulk of the paper.

Our main contributions are: (i) In Section 2 we present a novel algorithm and software which efficiently and provably accurately (see Section 3) calculates the number of most likely physical error configurations that cause logical errors for any d . One can then plug in any p to obtain the corresponding logical error rates. (ii) In Section 3, we prove a limitation on predicted scaling of logical error rates given p, d [5] to p, d such that $pd^2 \ll 1$. This limitation has not yet been shown by experiments, because d is too small on real quantum hardware. We prove that $pd^2 \ll 1$ is sufficient for the most likely configurations to be the only ones who contribute meaningfully to the logical error rate (the approximation in Section 2). (iii) In Section 4, we show that taking a number of measurements equal to d is sufficient to make measurement errors negligible for rotated surface codes. (iv) In Section 5, We extend our model to particular correlated or anisotropic noise. Section 6 summarizes our work and proposes future research directions.

Table 1. Notation, not including notation specific to [Section 4](#) or [Section 5](#).

Variable	Meaning	Function relations
d	code distance	$d\%2 = 1$
p	physical error rate	
L	logical error rate	$L = f(p, d)$ - goal is to determine $f()$
C_k	# configurations of k physical errors resulting in logical error	$C_k = g(d)$ - goal is to determine $g()$
P_k	probability of k physical errors resulting in logical error	$P_k = h(p, d)$ - goal is to determine $h()$
d_e	minimum # of physical errors required for a logical error	$d_e \doteq (d + 1)/2$
p_{th}	threshold below which L decays exponentially in p	$p_{th} > p$

2. The minimum-length logical path (MLLP) problem

We consider a surface code with d^2 data qubits, where each qubit experiences an independent and identically distributed (i.i.d.) error with probability p . Throughout this paper, we assume d is odd. Our objective is to derive a provably accurate approximation for L . We can use this form to calculate error rates for logical qubits with small p . Additionally, we can use modifications to it to model measurement errors ([Section 4](#)), correlated errors, and anisotropic errors ([Section 5](#)). The logical error rate is

$$L = \sum_{k=0}^{d^2} C_k p^k (1-p)^{d^2-k} \doteq \sum_{k=0}^{d^2} P_k, \quad (1)$$

where C_k is the number of distinct physical error configurations involving k qubits that result in a logical error. Logical failures occur only when errors collectively form a path that is equivalent to a logical operator. For a surface code of distance d , this requires at least $k \geq (d + 1)/2 \doteq d_e$ physical errors. Consequently, $\forall k < d_e, C_k = 0$. An MLLP has length exactly d and produces a logical error if it has exactly d_e errors.

2.1. Unrotated codes

For unrotated codes, the only subsets of d physical qubits that fail to support d_e errors without inducing a logical error are columns (for X -type errors) and rows (for Z -type errors). If the physical noise model includes X and Z -errors on each qubit (i.e., Y errors up to a phase), then C_{d_e} is exactly doubled by symmetry. Doubling does not introduce over-counting, because a given error path cannot simultaneously be an X -type and a Z -type logical path; the two classes of paths are topologically and syndrome-wise disjoint. Without loss of generality (**wlog**), we restrict attention to X -errors.

$$C_{d_e} = d \binom{d}{d_e} = \frac{d}{2} \binom{d+1}{d_e} \approx \frac{d/2}{\sqrt{\pi d_e}} 2^{d+1} \lesssim \sqrt{\frac{d_e}{\pi}} 4^{d_e}. \quad (2)$$

The simplifications in Eq. (2) come from the derivations

$$\binom{2n}{n} = \frac{2n!}{n!n!} \approx \frac{\sqrt{2\pi 2n} \left(\frac{2n}{e}\right)^{2n}}{\left(\sqrt{2\pi n} \left(\frac{n}{e}\right)^n\right)^2} = \frac{1}{\sqrt{\pi n}} 2^{2n}, \quad (3a)$$

$$\binom{2n-1}{n} = \frac{(2n-1)!}{n!(n-1)!} = \frac{1}{2} \frac{2n(2n-1)!}{n!n(n-1)!} = \frac{1}{2} \frac{2n!}{n!n!} = \frac{1}{2} \binom{2n}{n} \quad (3b)$$

We use Stirling's approximation in Eq. (3a) to show agreement with the scaling law [5]

$$L \approx A \left(\frac{p}{p_{th}} \right)^{d_e}. \quad (4)$$

2.2. Rotated codes

For rotated codes, C_{d_e} is the number of ways d_e physical errors can occur along an MLLP that traverses the lattice horizontally (for Z -errors) or vertically (for X -errors). For example, in Fig. 1 $d = 5$, so any three errors on an MLLP will produce a logical fault. We will therefore count the number of such error configurations and use it to approximate L . Fig. 2 illustrates how a configuration with three errors can be mistaken for the more likely configuration containing only two errors on the same chain. X (Z)-error chains pass only through green (pink) squares.

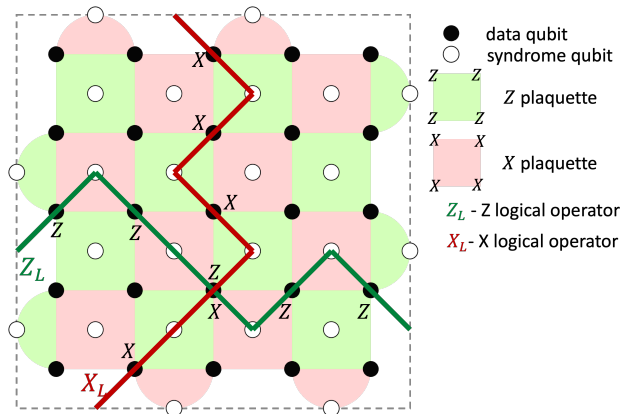


Figure 1. Rotated surface code that encodes a logical qubit using 25 data qubits and 24 syndrome qubits. X_L operators must pass through Z stabilizer plaquettes and Z_L operators must pass through X stabilizer plaquettes. An X (Z) error on a data qubit anticommutes with the neighboring Z (X)-type stabilizers and flips the parity (i.e., odd or even) of their measurement outcomes. An additional error on a data qubit adjacent to the same plaquette flips the parity of the syndrome qubit again, causing the error to go unnoticed (see Fig. 2.)

We build upon the approach in [1] of counting paths to estimate the logical error rate. Focusing on X -errors only, we obtain the following upper bound on C_{d_e} :

$$C_{d_e} \leq d 2^{d-1} \times \binom{d}{d_e} = \frac{1}{4} 2^{d+1} \times d \binom{d}{d_e} \leq \sqrt{\frac{d_e}{16\pi}} 16^{d_e}. \quad (5)$$

$d 2^{d-1}$ is an upper bound on the number of MLLPs. The path may start at any of the d boundary points and may proceed in at most two different ways at each of the

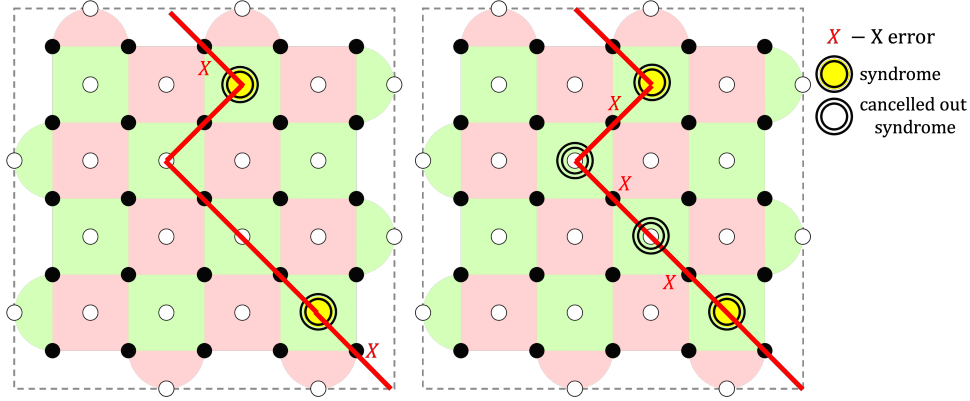


Figure 2. The configuration on the left is more likely because it has fewer errors. However, the decoder cannot distinguish these two configurations. So, if the configuration on the right occurs, the decoder will incorrectly identify it as the configuration on the left and apply the wrong correction. This results in a logical error.

subsequent $d - 1$ steps. This estimate is asymptotically tight because, as d grows, an increasing fraction of these paths remain entirely in the interior of the code and thus experience no boundary-induced constraints. Fig. 3 demonstrates the accuracy of $d2^{d-1}$ as the approximation of the number of paths, denoted by N_{paths} .

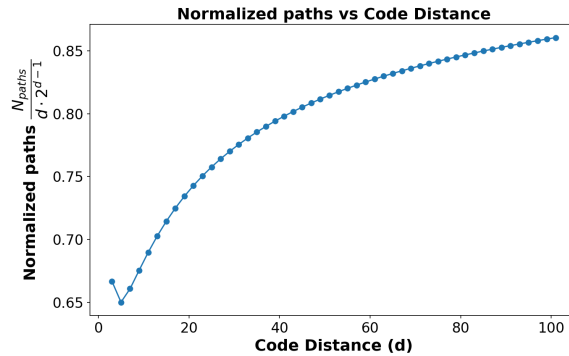


Figure 3. Approximating the number of paths N_{paths} as $d2^{d-1}$ becomes increasingly tight asymptotically.

The second term in Eq. (5) counts the number of ways to arrange errors along an MLLP. This approximation is a union bound because a fixed set of physical error locations may lie on multiple distinct MLLPs, causing such configurations to be counted more than once. As Fig. 3 indicates, any asymptotic divergence between the upper bound and the true value of C_{d_e} must originate entirely from this union-bound.

Similarly, we obtain the following lower bound to C_{d_e} :

$$C_{d_e} \geq \frac{Cd2^{d-1} \times \binom{d}{d_e}}{2^{d_e-1}} = \frac{C2^{d_e}}{2} \times d \binom{d}{d_e} \geq \sqrt{\frac{d_e}{16\pi}} 8^{d_e}. \quad (6)$$

The main difference from Eq. (5) arises from dividing by 2^{d_e-1} , the maximum number of MLLPs that can contain the same set of physical errors. The constant $C > 0.6$ reflects the edge effects, which become increasingly negligible as d increases (see Fig. 3). The gap between the bounds is large, so we turn to the precise geometric conditions

under which a logical error arises.

Theorem 1. *Precisely d_e physical errors produce a logical error if and only if one of two conditions hold for every pair of physical errors that is consecutive vertically:*

- *They are closer vertically than they are horizontally.*
- *They are diagonal on the grid (equidistant vertically and horizontally) and the diagonal path connecting them passes only through green plaquette(s).*

Proof. True by construction of MLLPs on rotated codes [2, 6, 11]. See also Fig. 2. \square

The code we provide in [this Github repository](#) computes C_{d_e} exactly and independently of p . Algorithm 1 provides a simplified overview of this method. The results agree with Eq. (4) when $A \approx 2.09 \cdot 10^{-1}$ and $p_{th} \approx 7.33 \cdot 10^{-2} \doteq p_{t-r}$. Fig. 4 shows this agreement for $p = 10^{-4}$. Our upper bound given in Eq. (5) corresponds

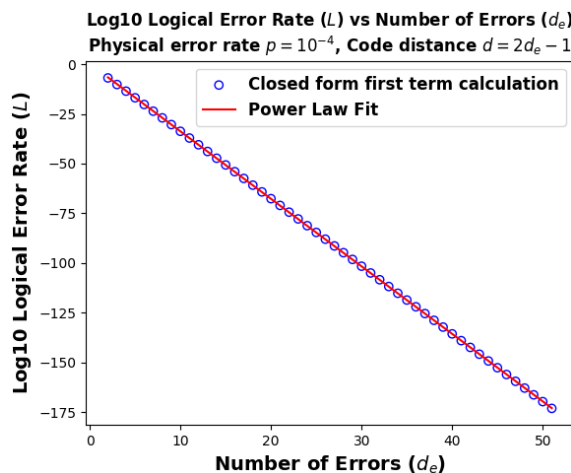


Figure 4. The code agrees with Eq. (4) with $A \approx 2.09 \cdot 10^{-1}$ and $p_{th} \approx 7.33 \cdot 10^{-2}$ ($R^2 = 1 - 6.32 \cdot 10^{-6}$).

to $A \approx 4.04 \cdot 10^{-1}$ and $p_{th} \approx 6.22 \cdot 10^{-2}$. Our lower bound in Eq. (6) corresponds to $A \approx 4.04 \cdot 10^{-1}$ and $p_{th} \approx 1.24 \cdot 10^{-1}$. Asymptotically, the upper bound is substantially closer than the lower bound with respect to the actual count.

We fit Eq. (2) to Eq. (4) and get $A \approx 1.62$ and $p_{th} \approx 2.49 \cdot 10^{-1} \doteq p_{t-ur}$ for the unrotated code. For a given distance, this is substantially better than the rotated code, but rotated code can have a distance larger by a factor of $\approx \sqrt{2}$. We compare the two and see that if $p^{(\sqrt{2}-1)d_e} \lesssim 7.75 p_{t-r}^{\sqrt{2}d_e} / p_{t-ur}^{d_e}$, the rotated code has lower logical error rates per qubit count. This gives a closed form for the experimental results from [11] and shows the limits of extrapolating them in certain regimes.

3. Relationships between coefficients

Theorem 2. $\forall k \geq 0, C_{d_e+k} \leq \binom{d^2-d_e}{k} C_{d_e} \leq \frac{d^{2k}}{k!} C_{d_e}$.

Proof. Any configuration with d_e physical errors that creates a logical error can have errors arbitrarily added anywhere on the surface and will create a logical error if there are no error cancellations. There are $d^2 - d_e$ locations for these next errors and the inequality comes from the locations that result in error cancellation. Any set of k errors

Algorithm 1 Count Error Patterns - see code [here](#)

```
1: function IsValidTransition(prev_row, prev_col, row, col)
2: if row ≤ prev_row then
3:   return false
4: end if
5: dx ← col − prev_col, dy ← row − prev_row
6: if dy < |dx| then
7:   return false
8: end if
9: if dy = |dx| then
10:  if (row + col)%2 == 0 and dx < 0 then
11:    return false
12:  end if
13:  if (row + col)%2 == 1 and dx > 0 then
14:    return false
15:  end if
16: end if
17: return true
18:
19: function CountMLLP(d, curr_row, curr_col, rem_errs)
20: if rem_errs = 0 then
21:   return 1
22: end if
23: if state is memoized then
24:   return memoized value
25: end if
26: count ← 0
27: for next_row = curr_row + 1 to d − 1 do
28:   for next_col = 0 to d − 1 do
29:     if IsValidTransition(curr_row, curr_col, next_row, next_col) then
30:       count ← count + CountMLLP(d, next_row, next_col, rem_errs − 1)
31:     end if
32:   end for
33: end for
34: memoize count
35: return count
36:
37: function CountErrorPatterns(d, n)
38: total ← 0
39: for start_row = 0 to d − n do
40:   for start_col = 0 to d − 1 do
41:     total ← total + CountMLLP(d, start_row, start_col, n − 1)
42:   end for
43: end for
44: return total
```

that did not create a logical error, but then did when an error was added is accounted for, by switching this last error with one that was not in the error path. The second inequality comes from $d^2 - d_e < d^2$ and Eq. (3) in [3]. \square

It follows that $\forall k \geq 0$

$$P_{d_e+k} < \frac{(d^2 p)^k P_{d_e}}{k!}. \quad (7)$$

Therefore, the P_k s decay exponentially if $pd^2 < 1$. So when $pd^2 \ll 1$, $L \approx P_{d_e}$. The inequality in Eq. (7) becomes looser as k and the probability for error cancellation increase, making the approximation $L \approx P_{d_e}$ even better. This confirms the quality of Eq. (4) in this regime. Fig. 5 shows a lower bound on the multiplicative correction factor to $L \approx P_{d_e}$. The contribution of P_{d_e+1} is substantial in certain regimes.

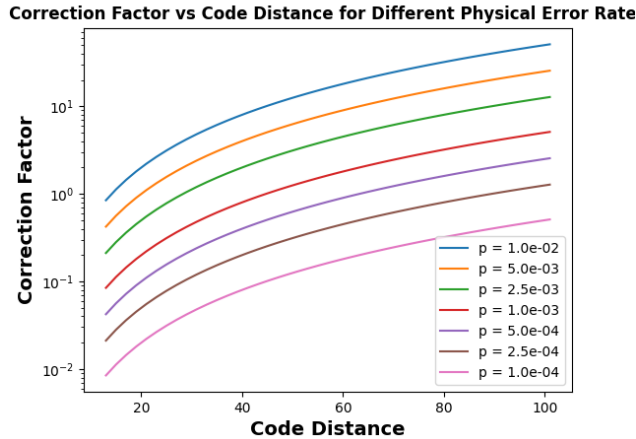


Figure 5. The correction factor P_{d_e+1}/P_{d_e} increases with the code distance d and physical error rate p .

However, if $k \ll d^2$, most locations of a $k + 1$ -th error will not result in error cancellation. This means $0.5d^2 p P_{d_e} < P_{d_e+1} < d^2 p P_{d_e}$. In the regime $pd^2 \gtrsim 1$, this contradicts the assumption that d_e errors leading to a logical error are more likely than $d_e + 1$ errors doing so [5]. This could result in less favorable scaling if $pd^2 \gg 1$.

Deriving a general lower bound on P_{d_e+k} is more complicated for $k > 1$ because one error could cancel another error in the path, but another error could recomplete the path. This makes the P_k s decay eventually, but it is challenging to calculate precisely when. We leave this analysis for future work, as current surface codes have $pd^2 \ll 1$.

4. Measurement errors

Our analysis so far neglected measurement errors on the ancilla qubits for correction. We can repeat each calculation some odd $M \geq 3$ times independently, measure each time, and majority vote to decide the correct value of the ancilla qubit. We define $M_e \doteq (M + 1)/2$. If we have $< M_e$ measurement errors on an ancilla qubit, we can trust it to perform as expected. Let p_M be the probability that a given ancilla qubit has $\geq M_e$ measurement errors. We assume that a logical error due to measurement errors occurs if and only if at least one ancilla qubit has $\geq M_e$ measurement errors. This approximation is good when $p_M d^2 \ll 1$, because measurement errors are unlikely to occur on multiple qubits in precisely a way that cancels out.

We follow the approach in [4], extending time to a third (upward Z) dimension of our surface code. A logical error occurs when a majority of qubits in a tube parallel to the

Z axis error. This behavior is identical to the other 2 dimensions in the unrotated code [4], but different than in the rotated code. Assuming the probability for a measurement error on any qubit is p_m i.i.d, M measurements are taken on each ancilla, and $N_a = \Omega(d^2)$ is the number ancilla qubits,

$$L_M = 1 - \left[1 - \sum_{k=M_e}^M \binom{M}{k} p_m^k (1-p_m)^{M-k} \right]^{N_a} \doteq 1 - [1 - p_M]^{N_a}. \quad (8)$$

If $p_m \ll 1$, $p_M \approx \binom{M}{M_e} p_m^{M_e} (1-p_m)^{M_e-1}$ because $\forall m \geq M_e$, $\binom{M}{m} \geq \binom{M}{m+1}$. If $N_a p_M \ll 1$, $L_M \approx N_a \binom{M}{M_e} p_m^{M_e}$. We use Eq. (3), to get $L_M \approx N_a (4M_e \pi)^{-0.5} (4p_m)^{M_e}$.

We want to select M such that measurement errors are less frequent than data errors. For an unrotated code, based on Eq. (2), $L_{ur} \approx \sqrt{\frac{d_e}{\pi}} (4p)^{d_e}$. The exponential scaling in d_e is identical to that of L_M , but the polynomial term is smaller. For rotated code, based on Fig. 4 and our code, $L_r \approx A(p/p_{th})^{d_e}$ with $A \approx 2.09 \cdot 10^{-1}$ and $p_{th} \approx 7.33 \cdot 10^{-2}$. The exponential scaling in d_e has a larger base.

For given p , p_m , d , we can calculate the necessary M to ensure $L_M < L$. $M = d$, and $p_m = p$ is a particularly interesting case, because the dependence on p , p_m vanishes. We compare the terms and conclude that $\forall p$ (that fulfills our other assumptions) $M = d$ is insufficient for $L_{ur} < L_M$, but sufficient for $L_r < L_M$.

5. Design implications

5.1. Global correlated errors

We can extend the approximation of the logical error to a simple global correlated model. Suppose that instead of p being drawn from a Bernoulli distribution, it is drawn from one of D Bernoulli distributions, each occurring with a certain probability **for all qubits simultaneously**. Meaning

$$p_{dep} = \sum_{j=1}^D \rho_j p_j, \quad \sum_{j=1}^D \rho_j = 1 \quad (9)$$

where ρ_j is the probability of the j th distribution occurring, and p_j is the physical error rate associated with that distribution. This type of distribution models errors occurring due to unfavorable environments such as those with fluctuating temperatures, manufacturing line defects, or in the presence of cosmic rays [8]. The form for the logical error is in this case:

$$L_{dep} = \sum_{k=d_e}^N C_k \sum_{j=1}^D \rho_j p_j^k (1-p_j)^{N-k}. \quad (10)$$

Wlog, we can assume $\forall j p_j > p_{j+1}$. Unless ρ_1 is very small, i.e. $\exists j$ where $\rho_1 p_1^{d_e} < \rho_j p_j^{d_e}$, we see that $j = 1$ dominates the rest of Eq. (10). In any case, there is some d beyond which $j = 1$ dominates the sum. Therefore, the scaling of any logical qubit error rate is dominated by p_1 at large enough code-distances, modulated by ρ_j . Quantum computer

designers should therefore consider worst-case, rather than mean or median, physical error rates when designing error correcting codes.

5.2. Different X and Z error rates

Here we shift our discussion to rectangular rotated surface codes which require hw physical data qubits, and $hw - 1$ syndrome qubits used for measurements. Here, h is the surface code's height and w is its width. So the total number of qubits required is $2hw - 1$. The remaining unconstrained value is the logical qubit.

Consider some budget of Q qubits for a logical qubit. If the probability for a physical X and Z error are equal ($p_x = p_z$), we can choose $w = \lfloor \sqrt{(Q+1)/2} \rfloor$. If $2w(w+1) - 1 \leq Q$, we choose $h = w + 1$, otherwise, $h = w$. Wlog, we can switch w and h .

Assume wlog that $p_x \geq p_z$ and denote by L_x and L_z the probability for logical X and Z errors. We can start by using the values in Fig. 4 for A and p_{th} and plugging in p_x and p_z for p and $h = w = \lfloor \sqrt{(Q+1)/2} \rfloor = d$ to find d_e . In this case, $L_x \geq L_z$. Increase h by 1 and decrease w if necessary to remain within the qubit budget. Note the value of $L \doteq L_x + L_z - L_x L_z$, the total logical error probability. Repeat this until $L_x \leq L_z$ and note L 's value for that step as well. Choose the configuration that corresponds to the minimum L . This should occur in one of the last two steps, when $L_x \approx L_z$.

6. Summary and future work

We introduce a novel recursive algorithm for calculating logical error rates for rotated codes when $pd^2 \ll 1$ by counting MLLPs. It calculates C_{d_e} as a function of d , but runs in seconds even for large d . We can plug the result for any p into Eq. (1). When $pd^2 \gtrsim 1$ it provides a lower bound to the logical error. We explicitly derive the regime in which rotated codes are better than unrotated codes. We explain how to use these calculations to account for measurement errors and design practical QEC surface codes.

Our method of counting configurations is only valid when the qubits are identical, but it is not necessary for them to be independent. Future work may consider more general qubit dependencies in space and time, along with more general measurement errors. Further research is also needed to see if Algorithm 1 can be extended to count C_k for at least some of the first k s where $k > d_e$. This will extend the p and d regime in which an approximation such as Algorithm 1 is accurate. This recursive counting method may also be useful for combinatorial problems in other domains.

Acknowledgements

This research was funded by the DARPA Microsystems Technologies Office's Quantum Benchmarking Initiative, contract number O2508-097-089-117256. The views, opinions and/or findings expressed are those of the authors and should not be interpreted as representing the official views or policies of DARPA or the U.S. Government.

References

- [1] Panos Aliferis, Daniel Gottesman, and John Preskill. Accuracy threshold for postselected quantum computation. *Quantum Info. Comput.*, 8(3):181–244, March 2008.

- [2] H. Bombin and M. A. Martin-Delgado. Optimal resources for topological two-dimensional stabilizer codes: Comparative study. *Phys. Rev. A*, 76:012305, 2007.
- [3] Shagnik Das. A brief note on estimates of binomial coefficients, 2016.
- [4] Eric Dennis, Alexei Kitaev, Andrew Landahl, and John Preskill. Topological quantum memory. *Journal of Mathematical Physics*, 43(9):4452–4505, 2002.
- [5] Austin G. Fowler, Matteo Mariantoni, John M. Martinis, and Andrew N. Cleland. Surface codes: Towards practical large-scale quantum computation. *Physical Review A*, 86(3), 2012.
- [6] Dominic Horsman, Austin G. Fowler, Simon Devitt, and Rodney Van Meter. Surface code quantum computing by lattice surgery. *New Journal of Physics*, 14:123011, 2012.
- [7] A.Yu. Kitaev. Fault-tolerant quantum computation by anyons. *Annals of Physics*, 303(1):2–30, 2003.
- [8] X. Li, J. Wang, YY. Jiang, et al. Cosmic-ray-induced correlated errors in superconducting qubit array. *Nature Communications*, 16:4677, 2025.
- [9] Ashley Montanaro. Quantum algorithms: an overview. *npj Quantum Information*, 2, 2016.
- [10] Michael A. Nielsen and Isaac L. Chuang. *Quantum Computation and Quantum Information: 10th Anniversary Edition*. Cambridge University Press, 2010.
- [11] Anthony Ryan O’Rourke and Simon Devitt. Compare the pair: Rotated versus unrotated surface codes at equal logical error rates. *Phys. Rev. Res.*, 7:033074, 2025.